IET Renewable Power Generation

Special Issue Call for Papers

Be Seen. Be Cited. Submit your work to a new IET special issue

Connect with researchers and experts in your field and share knowledge.

Be part of the latest research trends, faster.

Read more

Conjugate refractive–reflective homogeniser in a 500× Cassegrain concentrator: design and limits

Katie Shanks[1] ✉, Hasan Baig[1], Sundaram Senthilarasu[1], K.S. Reddy[2], Tapas K. Mallick[1]

[1]*Environmental and Sustainability Institute, University of Exeter Penryn Campus, Penryn TR10 9FE, UK*
[2]*Heat Transfer and Thermal Power Laboratory, Department of Mechanical Engineering, Indian Institute of Technology Madras, Chennai 600 036, India*
✉ *E-mail: kmas201@exeter.ac.uk*

Abstract: In this study, we present the conjugate refractive reflective homogeniser (CRRH) to be used in a 500× Cassegrain photovoltaic concentrator. The CRRH is a dielectric crossed v-trough lined with a reflective film whilst maintaining an air gap between them. This air gap between the two surfaces helps in trapping the scattered light from the refractive geometry and ensures both total internal reflection and standard reflection of the escaped rays. A 10–42% drop in optical efficiency has been shown to occur due to varying the surface roughness of the homogeniser in these ray trace simulations for the Cassegrain setup. The CRRH increased the overall optical efficiency by a maximum of 7.75% in comparison with that of a standard refractive homogeniser simulated within the same concentrator system. The acceptance angle and flux distribution of these homogenisers was also investigated. The simple shape of the CRRH ensures easy manufacturing and produces a relatively uniform irradiance distribution on the receiver. The theoretical benefit of the CRRH is also validated via practical measurements. Further research is required but a 6.7% power increase was measured under a 1000 W/m² solar simulator at normal incidence for the experimental test.

1 Introduction

There is a growing interest in concentration photovoltaic (CPV) technologies due to their reduced need for photovoltaic (PV) material and higher potential efficiencies. Not only can CPV systems be the answer to reducing the cost of solar power but they are also more environmentally friendly than regular flat plate PV panels. Two reasons for this are: first, CPV technologies use less semiconductor material and second they have a smaller effect on the albedo change in an area than that of flat plate PV panels [1–3]. The Albedo is the percentage of incoming radiation reflected off a surface. Covering surfaces with dark coloured flat plate PV panels results in absorbing and emitting more thermal energy if the original surface was not initially of a similar dark colour (e.g. fields). Owing to the relatively low efficiency of flat plate PV panels in comparison with CPV, they convert more of the incoming radiation into heat rather than electricity. This method of PV can change the overall albedo of an area, and contribute to the effect of 'urban heat islanding' [1–3]. Higher-efficiency technologies transfer less of the absorbed energy into heat and do not affect the albedo of an area as significantly as that of flat PV panels [3].

As the concentration ratio of an optic is increased, it becomes more difficult to maintain a high optical efficiency, uniform irradiance distribution, and an acceptable optical tolerance for the system simultaneously [4]. Matching the output irradiance size and shape to the receiver size and shape affects all of these factors and non-uniform illumination has a detrimental impact on the solar cell performance [5]. A secondary optic or homogeniser element improves this and is needed to relax the demand on the system's accuracy [6, 7]. Some secondary concentrator optics include the compound parabolic concentrator (CPC) [8], the dome lens [9], the ball lens [10] and various homogenising light funnel geometries [11–13]. These typically take on the shape of an inverted cone or pyramid but there are also elliptical and hyperbolic optics possible [8, 14, 15].

One key consideration in all of the above named designs is the material to be used and the resulting surface quality. The surface

roughness of total internal reflection (TIR) optics causes scattering of incoming light, reducing its performance from the ideal design.

Glass is typically the best choice for high-quality accurate optics but the strength, flexibility and light weight of plastics make polymers such as Polymethylmethacrylate (PMMA) the more economic option. PMMA is the most popular polymer used in CPVs and polyethylene is used widely in other areas but has a short lifetime. Polyamide, polystyrene, acrylics and polycarbonate have been investigated but more research is required [16]. Lenses may be manufactured by hot-embossing, casting, extruding, laminating, compression-moulding or injection-moulding thermoplastic PMMA [17]. Reflective optics also depend greatly on their surface quality. A silvered mirror using smooth glass produces a common mirror with reflectivity >85% but complex shapes are difficult and expensive. Reflective films are an alternative simple and effective option for reflective-based optics. They are lightweight, typically cheaper than solid polished metals and films with >90% reflectivity are available. Their application to surfaces, especially three-dimensional (3D) curves, can be difficult however [18]. Polymer mirror films are a more recent low-cost, low-weight option to gain >90% reflective surfaces but require specially designed structures to gain the correct shape [19, 20]. In terms of mirrors, vacuum metallising is the current best option but this process, such as refractive lenses, is again highly dependent on the material and surface quality [21, 22].

The surface structure of an optical element or the interface between two optical mediums, has a strong influence on the final direction of the reflected or refracted light. During design simulations, these optical surfaces are sometimes assumed ideally smooth with no scattered light losses. There is however no ideally smooth optical surface for lenses or mirrors and an inherent roughness is always present. The degree of this surface inhomogeneity depends on the manufacturing process and material used with higher-quality optical finishes and coatings costing more [23]. Manufacturing processes for optics include precise grinding, milling, polishing and a variety of coating methods for a smooth finish. Computer-controlled diamond turning machines, as well as

other modern materials and moulding techniques, have significantly improved the design and accuracy of refractive optics such as Fresnel lenses [24]. Similarly, computer-aided design and machining has improved the quality of reflective optics but in both cases good-quality prototyping can be expensive when requiring smooth and accurate geometries. Simple cost effective methods to improve the optical efficiency of optics are needed, whether the design is in a prototyping or final installation stage. There are several methods to measure the optical scattering of a surface, and hence various terms associated with its severity [25, 26]. Here, we will refer to the bidirectional scattering distribution function (BSDF) which is associated with the surface roughness of optical interfaces through the total integrated scatter and dictates how light is transmitted or reflected from it. The BSDF is the combined function of the bidirectional reflectance distribution function and the bidirectional transmittance distribution function. The BSDF is generally in the form of a mathematical formula, often encompassing discrete samples of measured data, which approximately models the actual surface behaviour. The BSDF radiometrically characterises the scatter of light from a surface as a function of the angular positions of the incident and scattered rays [27].

2 Design considerations

One commonly utilised and widely researched concentrator design is the Cassegrain concentrator which has the advantages of compactness and having an upward facing receiver [6]. With the receiver situated in the base of the primary reflector (see Fig. 1a), passive cooling methods are more easily employed and the cell temperature is more manageable. Surface imperfections however will reduce the optical efficiency at every stage. The primary and secondary dishes as shown in Fig. 1a will have an associated non-ideal reflectance. A reflective homogeniser optic would similarly suffer, especially if there are many reflections occurring within. A refractive medium takes advantage of TIR but again, surface roughness, scratches or any form of soiling is subject to refraction losses. This includes when the rays initially refract into the homogeniser and a small portion of energy is reflected instead of refracted. A simple but effective method to recover rays which fail TIR at the homogeniser walls is to use a reflective sleeve with an air gap [28] as shown in Figs. 1b and 1c. Baig et al. [29, 30] discuss the optical loss caused by the encapsulation medium used in connecting low-concentration optics to solar cells. Light rays incident in this overlap region do not reflect toward the solar cell but continue through the encapsulation medium until lost. Baig et al. [29, 30] overcame the encapsulation issue by adding a strip of reflective film to the bottom edge of the 3D cross CPC designed for building integration. We expand on this method by applying reflective film with an air gap to all of the TIR active walls of a homogeniser in a high-concentration Cassegrain concentrator. Hence, the conjugate refractive–reflective homogeniser (CRRH) is presented.
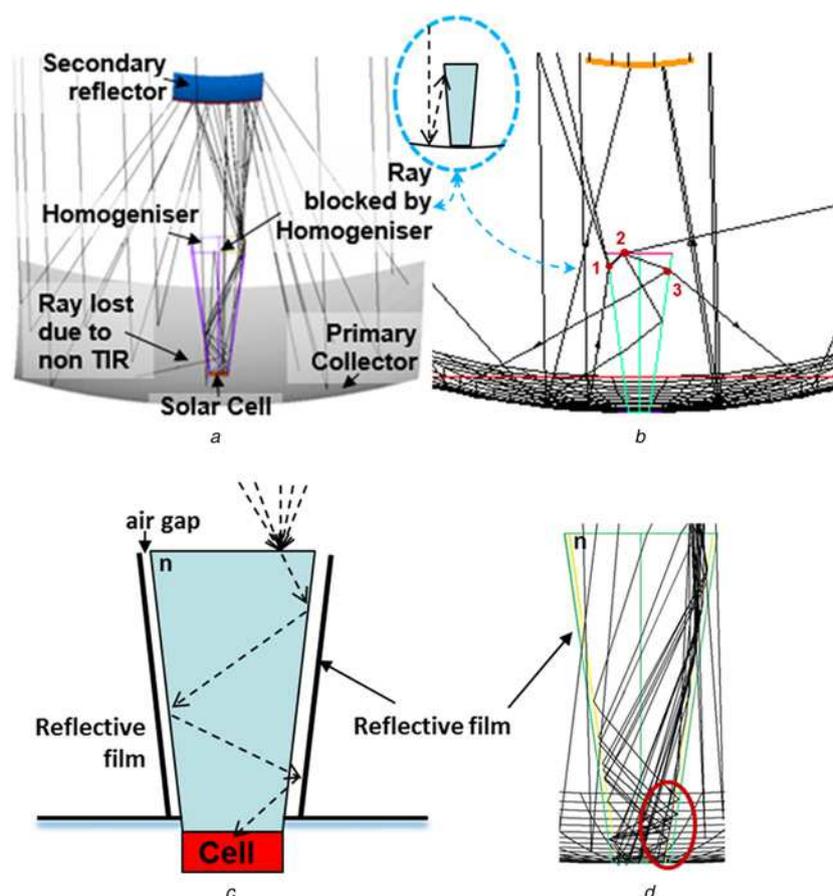
Fig. 1 *Design considerations*

a Ray trace simulation of Cassegrain concentrator at a tracking error of ±1.75°. Lost rays are shown including an inlet diagram of how a light ray can be blocked by the homogeniser on route to the secondary reflector. This 'blocked' ray can take various routes as shown in (b)

b Ray trace simulation showing possible processes of intercepted ray at homogeniser interfaces indicated by nodes 1, 2 and 3. At node 1, an intercepted ray from the primary reflector is either scattered away from the homogeniser and lost upwards or refracted into the homogeniser depending on the materials refractive index and surface structure. At node 2, the light can again either be scattered out of the homogeniser or scattered within the homogeniser. In reality, a number of rays would be dispersed in many directions at each node but only a few are shown here. Again each of these rays can be reflected or refracted when incident on the homogenisers' walls as shown at node 3. It is possible that some of these rays find their way to the cell, though from the results obtained in these experiments their contribution is negligible

c Theoretical performance of CRRH with air gap between reflective films

d Ray trace diagram confirming that refracted rays can be caught by the reflective film (thick red circle)

2.1 Parameters and limitations

A previous study has been carried out to determine the dimensions of the primary and secondary reflectors as well as the homogeniser dimensions [31]. Overall, the design has a good acceptance angle of >1°. The homogeniser geometry is set such that a perfect surface should only loose a negligible percentage of energy due to light rays not meeting TIR (>0.01%). When increasing the misalignment with the Sun up to 2° an increase in light loss occurs in this design due to interception by the homogeniser after reflection from the large primary mirror (Figs. 1a and 1b) which increases loss. At <0.5°, misalignment of this loss is almost negligible but increases up to ~1.7% at ±2° solar misalignment. This will limit the air gap and thickness of the reflective sleeve but would not be the case for other designs such as the Fresnel lens. In this paper, simulations with an increasing air gap between the refractive homogeniser surface and reflective film surface (Figs. 1b and 1c) were carried out. The solar cell size was 1 cm × 1 cm and the geometrical concentration ratio was 500×.

3 Simulation method

Simulations were carried out using Breault's Advanced System Analysis Program (ASAP) ray tracing software. The source was set to imitate energy from the Sun with 1000 W/m² and a divergence angle of ±0.27°. The homogeniser material is set as SHOTT BK7, with a dispersion curve as shown in Fig. 2. This is a commonly used medium and has a higher refractive index than others such as PMMA. The homogeniser will be made out of a material with a similarly stable and high refractive index to SHOTT BK7 (to improve TIR within).

For measurements of the air gap thickness, the BSDF of the homogeniser was chosen to be similar to that of standard polished aluminium, following the Harvey model. This model was chosen as the homogeniser will be moulded from an aluminium casing with polished inner surfaces.

Simulations were carried out assuming first the scenario of perfect surface qualities and 100% reflectance for reflectors and 0% absorbance for the homogeniser. About ~10% reflectance loss is then assumed for the two reflective dishes assuming their surfaces follow the polished mirror BSDF (Fig. 3a). The losses incurred when the light rays refract into the homogenisers entry aperture and are absorbed are included next and finally a surface roughness is added to the homogeniser material. A selection of BSDFs were used in the simulations for this investigation, their plots are given in Fig. 3 and all taken from the Breault software ASAP scattering
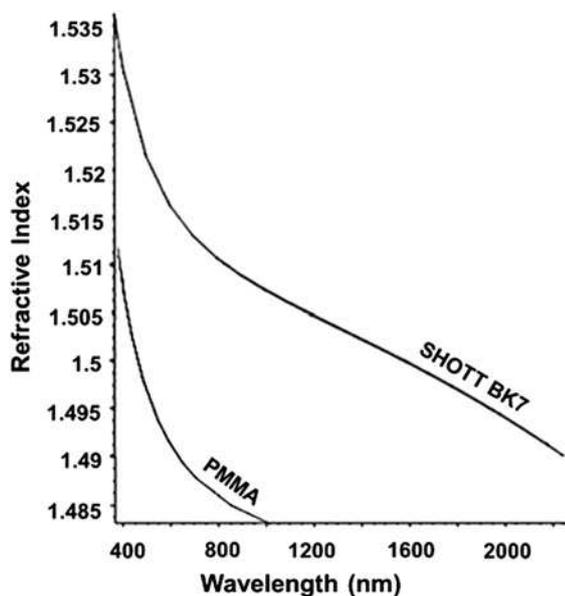

Fig. 2 *Dispersion functions of PMMA and SHOTT BK7*

library [32]. For these simulations a modified Harvey model was used with the selected BSDFs and though the BSDF cannot fully be shown with any 2D or 3D graph the curves in Fig. 3 are given as some indication of the light scattering profile. The graphs show the log BSDF versus the scattering angle (with respect to the specular angle) for three different incidence angles. All the scatter profiles follow the rule that most of the scattered light should be equal to the angle of incidence (the peaks shown in the graphs in Fig. 3). Differences can be seen in how the remainder of the light is distributed at non-specular angles (scattered) [27, 32]. The effects and contributions of these imperfect optical elements on optical efficiency and acceptance angle are given in Figs. 4 and 5.

Simulations were then carried out with the addition of a reflective film sleeve to the homogeniser at increasing air gap widths to investigate its advantages.

4 Results and discussion

4.1 Optical efficiency decrease in realistic system

Fig. 4 confirms that no light rays are lost within the system at normal incidence as shown by the 'ideal' scenario results.

As can be seen from Figs. 4 and 5, the addition of a 10% reflection loss on both dishes causes a significant drop in optical efficiency. There are materials and coatings with improved reflectance [16] such as silver (~97% reflectance) but degradation and/or expense are common problems with such high-quality reflective materials. All following simulations hence consider 90% reflective primary and secondary dishes so as final results are more realistic.

There is a small loss of energy due to when the light refracts into the homogeniser and some portion of the rays is reflected away. This can be improved with antireflection coatings and special textures of the homogeniser surface but again this is expensive [33, 34].

The surface roughness is a main factor causing a drop in optical efficiency and lowering the acceptance angle (Figs. 4 and 5). There is a severe drop especially for the BSDF's related to poorer surface finishes as shown in Fig. 4. These BSDF's were selected from a database of expected BSDF's of optical finishes available from companies. The BSDF's were chosen simply to give a good range. Typical surface quality would be expected to be in the upper region of these samples. Their effect is shown more clearly in Fig. 5 for the BSDF of polished aluminium, which though has the smallest drop in optical efficiency in Fig. 4, still contributes significantly to the total optical loss in Fig. 5. Owing to the increase in the solar misalignment angles, the rays reflect more within the homogeniser against the rough surfaced walls and are more likely to scatter instead of undergoing TIR. This causes the greater loss at >0.75° solar incident angles in Fig. 5. More accurate solar trackers and accurately built systems would not suffer as significantly if within ±0.5° accuracy but these incur further expense as well.

4.2 Impact of CRRH and air gap

Using first the lowest effecting BSDF (that of a standard polished aluminium) for the homogeniser surface and the added reflective film surface, an increase in optical efficiency was measured as shown in Fig. 6. The CRRH improves optical efficiency most between the 1° and 1.5° range of misalignment due to the increased incidence angle. When considering realistic conditions (90% reflectance from primary dishes and reflective film), the optical efficiency is increased by 2.8% (absolute value) at normal incidence and as high as 4.7% over the 1° and 1.5° regions as shown in Fig. 6. Though this is a significant gain, it should be noted that other manufacturing methods can result in smoother surface finishes with less light loss. The optical efficiency of any previous stage optics will also have an effect on the light saved by using the CRRH. If there is more energy going into the homogeniser, there is a greater portion of energy that can be trapped. The reflectance of the reflective film itself will alter
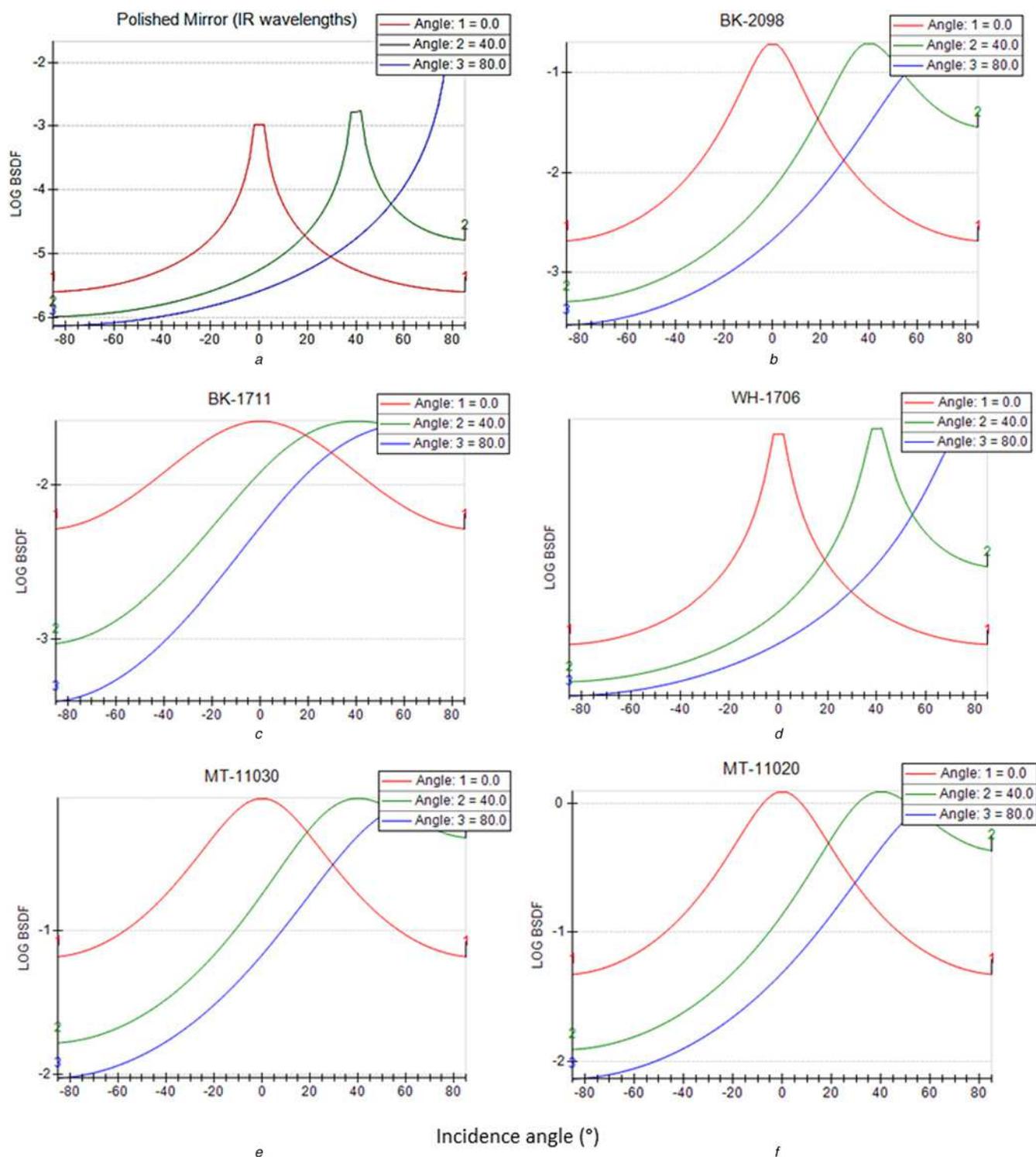
Fig. 3 *Logarithmic (LOG) BSDF against scatter angle from specular of*

a Polished mirror
b BK-2098
c BK-1711
d WH-1706
e MT-11030
f MT-11020

Three plots are shown in each graph for incidence angles of 0°, 40° and 80°. The BSDFs beginning with MT are representative of moulded optics surface profiles and those beginning with BK and WH are associated with specific materials available from lens providers. All plots were taken from the Breault ASAP scattering library [32]

results as well. If the CRRH with 0.01 mm air gap had 100% reflectance for the primary dishes and reflective film, the maximum optical efficiency gain would be ~7% for these simulations of a 500× Cassegrain system.

The thickness of the air gap was found to have very little effect on the efficiency with which refracted light rays are caught as shown in Fig. 7, though there is a significant difference without an air gap. Fig. 7 shows the optimum air gap to be 0.01 mm in these
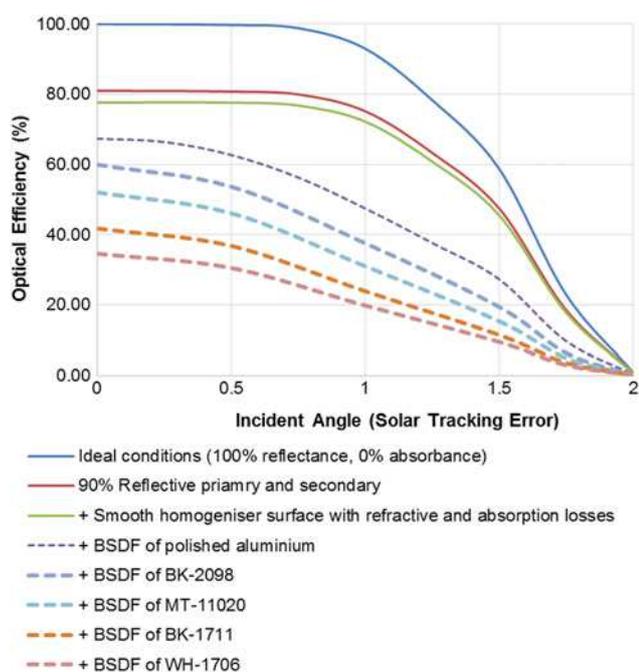
Fig. 4 *Practical losses summary. Optical efficiency decreases as surface losses are added in stages. The dashed lines represent possible surface finishes of the homogeniser depending on which material and manufacturing process is employed*

investigations. This would be nearly impossible to cost effectively implement due to manufacturing limitations but it can be assumed as small an air gap as is feasible considering manufacturing and cost would have the highest benefit.

Fig. 7 shows that with no air gap (0 mm), TIR is lost and all rays are reflected with specular losses (10%) in energy due to the 90% reflectance of the reflective film. As soon as there is an air gap, even as small as 0.01 mm in these simulations, the optical efficiency sharply increases as shown in Fig. 7. This increase in optical efficiency indicates how many reflections are experienced by the light rays, and hence the benefit TIR provides. The larger the increase in optical efficiency between the 0 and 0.01 air gap marks in Fig. 7, the more reflections occurring within the homogeniser which will benefit from TIR. This is why larger misalignment angles (except for 2° misalignment where most rays completely miss the homogeniser) have a more significant optical efficiency gain (vertical incline from 0 to 0.01 mm) in Fig. 7, because there are more reflections occurring.
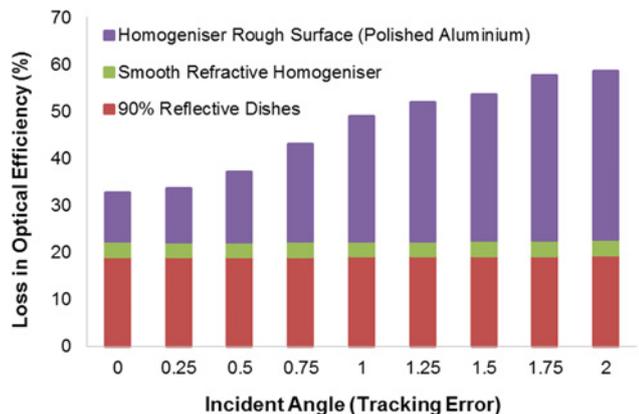
Fig. 5 *Contribution of optical losses from different imperfect surface considerations*

Thicker air gaps result in a longer path length of the non-TIR rays. This means rays will re-enter into the refractive medium at a lower position close to the solar cell and in theory possibly increase the optical efficiency of the system. However, in this Cassegrain design, a thicker air gap also blocks more rays travelling toward the secondary from the primary dish as mentioned earlier and as shown in Fig. 3. This would explain why there is a slight decrease in optical efficiency as the air gap thickness is increased in Fig. 7.

4.3 Impact of BSDF value

From the above results, it can be concluded that as small an airgap as possible is preferred. An air gap of 0.01 mm was hence used to investigate the effect of different BSDFs such as those already given in Figs. 3 and 4.

As can be seen from Fig. 8, the CRRH consistently improves the optical efficiency in comparison with a standard refractive homogeniser of this type for a range of surface scattering profiles. The maximum improvement is 7.75% with the BSDF of WH-1701 at normal incidence. Contrary to initial expectations however, this improvement did not increase with larger solar misalignment angles. At increased incident angles, the benefit of the CRRH decreased until negligible at 2° incidence angle as shown in Fig. 8 where the optical efficiency of the standard refractive homogeniser is almost zero. Misalignment with the Sun causes less light to reach the input surface of the homogeniser which can explain why the benefit of the CRRH decreases with increasing incidence angle. Also, if too many reflections occur within the homogeniser (due to the increased initial incidence angle), some light rays, despite being trapped at the CRRH walls, can still be reflected back out the entry aperture of the CRRH.

It can be drawn from these results that as long as there is some percentage (>2%) of light reaching the solar cell for the standard refractive homogeniser case, the CRRH will improve the optical efficiency by a non-negligible amount (as shown for the case of 1.75° incidence angle in Fig. 8). At normal incidence, the smallest optical efficiency improvement by the CRRH was 4.82% with a BSDF of BK-2098. These results confirm that the more efficient a purely refractive optic is to begin with (BK-2098 had the highest original optical efficiency as shown in Fig. 8), the less the addition of a reflective sleeve will improve the optical efficiency.

It should be noted that other manufacturing methods can result in smoother surface finishes with less light loss. The BSDFs beginning with MT in Figs. 3, 4 and 8 are representative of moulded optics surface profiles and those beginning with BK and WH are associated with specific materials available from lens providers.

4.4 Effect on irradiance distribution

The irradiance distribution on the solar cell is also affected by the surface roughness of the homogeniser as shown in Fig. 9.

The irradiance distribution is improved due to the slight diffusion of the rays from the rough surface of the homogeniser. In the case of the CRRH, when the reflective sleeve is added, the irradiance distribution is negligibly different to that without the reflective sleeve. The differences between the maximum and minimum irradiance values are given in Fig. 10. This shows a purely smooth and ideal optic to have the least homogeneous distribution, the addition of the rough surface modelling has the most homogeneous irradiance distribution and the CRRH has slightly less evenly distributed irradiance on the cell. As expected, with a higher misalignment angle, the distribution is less even, especially at 1°, before falling lower due to less total light being focused successfully to the solar cell.

4.5 Experimental validation

The measurements as shown in Fig. 11a gave a 3.5% current increase and a 6.7% power increase. When adding the reflective film to the refractive homogeniser (Figs. 11b and 11c), care was taken that the film did not optically stick to the refractive medium

IET Renew. Power Gener., 2016, Vol. 10, Iss. 4, pp. 440–447

444
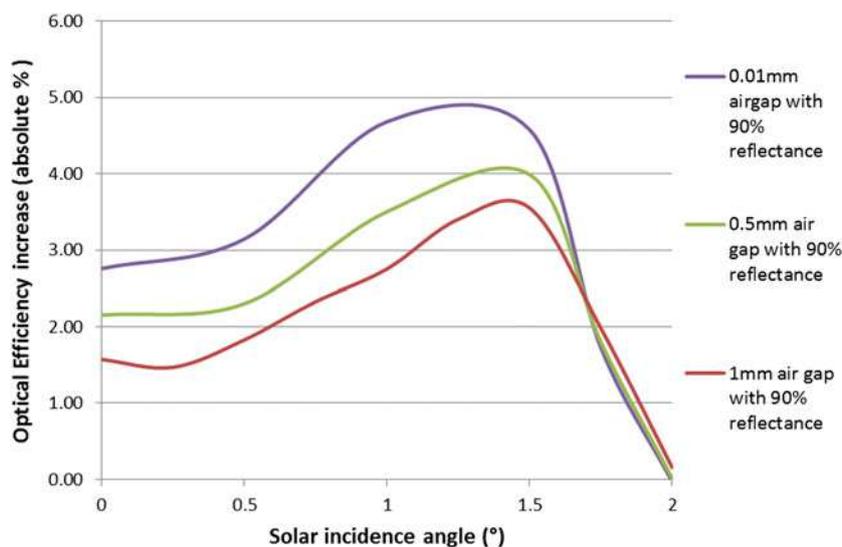
Fig. 6 *Increase in optical efficiency with the addition of the reflective sleeve under different conditions. Here, the base optical efficiency is that of the refractive homogeniser with the same dimensions and no reflective sleeve*
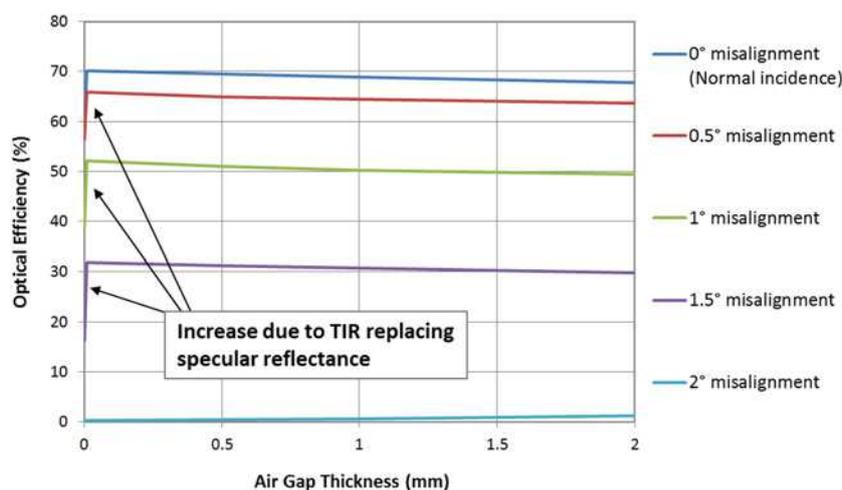

Fig. 7 *Graph of optical efficiency against air gap thickness for different solar misalignment angles*
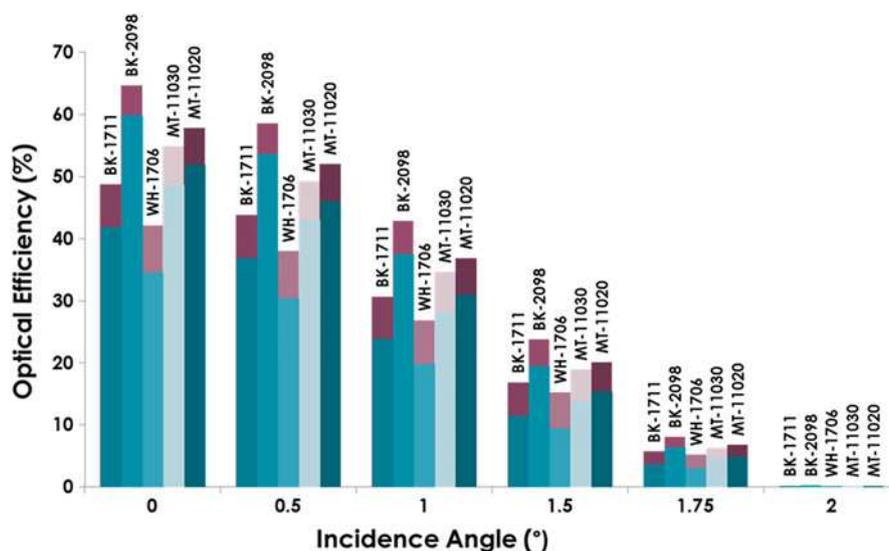
Fig. 8 *Increase in optical efficiency (purple shaded extensions at top of bars) due to the addition of the reflective sleeve to the refractive homogeniser with an air gap of 0.01 mm for increasing BSDF's. The incidence angle of the light is also increased up to 2° to show the effect misalignment has on the benefit of the CRRH in comparison with the performance of a refractive homogeniser (original blue shaded bars excluding extensions)*
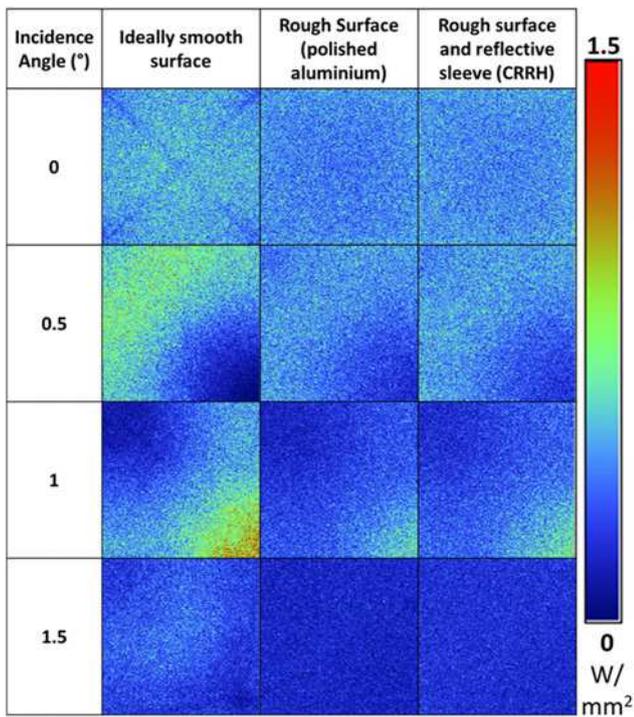
Fig. 9 *Irradiance distribution on solar cell with increasing solar incidence angle (increasing tracking error). Column 1: solar incidence angle on full Cassegrain system. Column 2: the case of 100% reflective dishes and a refractive homogeniser with an ideal surface finish. Column 3: results after the addition of a rough surface finish on the homogeniser. Column 4: same conditions as previous but with the reflective sleeve in place. The tracking error is set for both axes, hence the diagonal focusing*
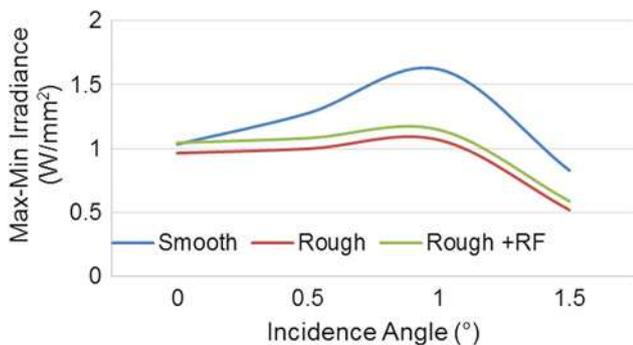

Fig. 10 *Irradiance range (max–min) on the solar cell with increasing solar incidence angle (increasing tracking error) for the smooth refractive homogeniser, the realistically rough refractive homogeniser and CRRH*

and prevent TIR. It was also ensured that the primary optic (Fresnel lens) only focused to the centre of the homogeniser for both tests and the same concentration ratio was maintained. With higher-efficiency primary optics and higher-concentration levels, the final stage optic gains more influence on the overall optical efficiency and performance. These practical measurements confirm the advantage of the CRRH over a plane refractive homogeniser.

5 Conclusion

The CRRH has been presented within the Cassegrain concentrator design. The CRRH has been shown to improve the optical efficiency by a maximum of 7.75% when considering a realistic surface roughness on the homogeniser and reflective optics within the Cassegrain concentrator system. The benefits of the CRRH are
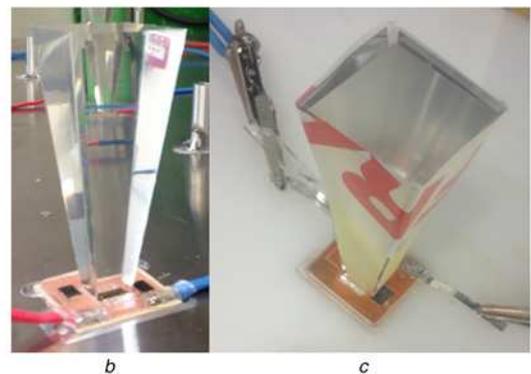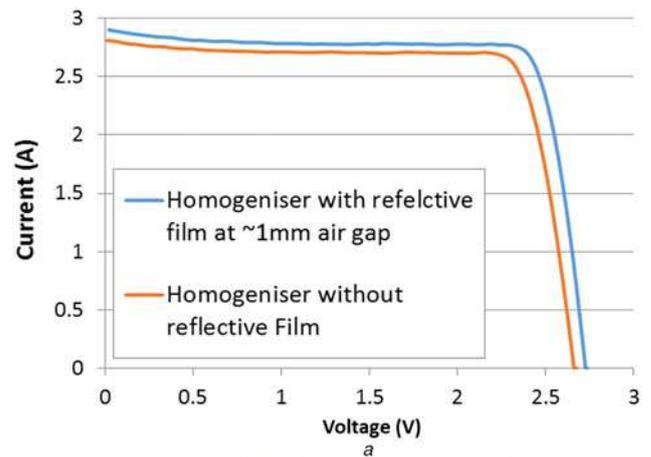
Fig. 11 *Experimental validation*
a I–V trace for the refractive homogeniser with and without the reflective sleeve and air gap
b Refractive homogeniser without reflective sleeve
c With reflective sleeve to make prototype CRRH

limited by the Cassegrain concentrator geometry and by the magnitude of surface roughness on the homogeniser. A high-quality homogenising optic with almost ideal surface smoothness would not benefit from the addition of a reflective sleeve but this is rarely the case due to difficult geometries and expense. Experimental tests confirmed the ray trace simulation analysis and a 6.7% performance improvement with the CRRH in comparison with the original refractive homogeniser was measured. Future work is required to fully understand the benefit conjugate refractive–reflective optics can have for solar concentrator technologies.

6 Acknowledgments

7 References

1 Akbari, H., Damon Matthews, H., Seto, D.: 'The long-term effect of increasing the albedo of urban areas', *Environ. Res. Lett.*, 2012, **7**, p. 024004
2 Gaffin, S.R., Imhoff, M., Rosenzweig, C., *et al*.: 'Bright is the new black – multi-year performance of high-albedo roofs in an urban climate', *Environ. Res. Lett.*, 2012, **7**, p. 014029

3   Burg, B.R., Selviaridis, A., Paredes, S., *et al*.: 'Ecological and economical advantages of efficient solar systems'. 'CPV-10', AIP Conf. Proc., 2014, pp. 317–320

4   Canavarro, D., Chaves, J., Collares-Pereira, M.: 'New second-stage concentrators (XX SMS) for parabolic primaries', comparison with conventional parabolic trough concentrators', *Sol. Energy*, 2013, **92**, pp. 98–105

5   Baig, H., Heasman, K.C., Mallick, T.K.: 'Non-uniform illumination in concentrating solar cells', *Renew. Sustain. Energy Rev.*, 2012, **16**, (8), pp. 5890–5909

6   Brunotte, M., Goetzberger, A., Blieske, U.: 'Two-stage concentrator permitting concentration factors up to 300× with one-axis tracking', *Sol. Energy*, 1996, **56**, (3), pp. 285–300

7   Canavarro, D., Chaves, J., Collares-Pereira, M.: 'New optical designs for large parabolic troughs', *Energy Procedia*, 2014, **49**, pp. 1279–1287

8   Winston, R., Miñano, J.C., Benítez, P., *et al*.: 'Nonimaging optics' (Elsevier, 2005)

9   Victoria, M., Domínguez, C., Antón, I., *et al*.: 'Comparative analysis of different secondary optical elements for aspheric primary lenses', *Opt. Express*, 2009, **17**, (8), pp. 6487–6492

10 Coughenour, B.M., Stalcup, T., Wheelwright, B., *et al*.: 'Dish-based high concentration PV system with Köhler optics', *Opt. Express*, 2014, **22**, (S2), p. A211

11 Araki, K., Leutz, R., Kondo, M., *et al*.: 'Development of a metal homogenizer for concentrator monolithic multi-junction-cells'. Conf. Record of the 29th IEEE Photovoltaic Specialists Conf., 2002, 2002, pp. 1572–1575

12 Gordon, J.M., Feuermann, D., Young, P.: 'Unfolded aplanats for high-concentration photovoltaics', *Opt. Lett.*, 2008, **33**, (10), p. 1114

13 Tang, R., Wang, J.: 'A note on multiple reflections of radiation within CPCs and its effect on calculations of energy collection', *Renew. Energy*, 2013, **57**, pp. 490–496

14 O'Gallagher, J., Winston, R.: 'No title test of a trumpet secondary concentrator with a paraboloidal dish primary', *Sol. Energy*, 1986, **36**, (1), pp. 37–44

15 Benítez, P., Miñano, J.C., Zamora, P., *et al*.: 'High performance Fresnel-based photovoltaic concentrator', *Opt. Express*, 2010, **18**, pp. A25–A40

16 Shanks, K., Senthilarasu, S., Mallick, T.K.: 'High-concentration optics for photovoltaic applications', in Pérez-Higueras, P., Fernández, E.F. (Eds.): 'High concentrator photovoltaics: fundamentals, engineering and power plants' (Springer International Publishing, 2015, 1st edn.), pp. 85–113

17 Leutz, R., Fu, L., Annen, H.P.: 'Stress in large-area optics for solar concentrators', in Dhere, N.G., Wohlgemuth, J.H., Ton, D.T. (Eds.): 'SPIE solar energy + technology' (International Society for Optics and Photonics, 2009), pp. 741206–741206–7

18 Jagoo, Z.: 'Tracking solar concentrators' (Springer Nether, 2013, 1st edn.)

19 Bader, R., Haueter, P., Pedretti, A., *et al*.: 'Optical design of a novel two-stage solar trough concentrator based on pneumatic polymeric structures', *J. Sol. Energy Eng.*, 2009, **131**, (3), p. 031007

20 Zanganeh, G., Bader, R., Pedretti, A., *et al*.: 'A solar dish concentrator based on ellipsoidal polyester membrane facets', *Sol. Energy*, 2012, **86**, (1), pp. 40–47

21 Barber, G.J., Braem, A., Brook, N.H., *et al*.: 'Development of lightweight carbon-fiber mirrors for the RICH 1 detector of LHCb', *Nucl. Instrum. Methods Phys. Res. A, Accel. Spectrom. Detect. Assoc. Equip.*, 2008, **593**, (3), pp. 624–637

22 Guo, S., Zhang, G., Li, L., *et al*.: 'Effect of materials and modelling on the design of the space-based lightweight mirror', *Mater. Des.*, 2009, **30**, (1), pp. 9–14

23 Yin, L., Huang, H.: 'Brittle materials in nano-abrasive fabrication of optical mirror-surfaces', *Precis. Eng.*, 2008, **32**, pp. 336–341

24 Leutz, R., Suzuki, A.: 'Nonimaging Fresnel lenses: design and performance of solar concentrators' (Springer Science & Business Media, 2001)

25 Kiontke, S. and Kokot, S.: 'Roughness reduction on aspheric surfaces,' in Classical Optics 2014, OSA Technical Digest (online) (Optical Society of America, 2014), paper OTu2B.4. doi:10.1364/OFT.2014.OTu2B.4 https://www.osapublishing.org/abstract.cfm?uri=OFT-2014-OTu2B.4

26 Brun, C., Buet, X., Bresson, B., *et al*.: 'Picometer-scale surface roughness measurements inside hollow glass fibres', *Opt. Express*, 2014, **22**, (24), p. 29554

27 Asmail, C.: 'Bidirectional scattering distribution function (BSDF): a systematized bibliography', *J. Res. Natl. Inst. Stand. Technol.*, 1991, **96**, (2), p. 215

28 Baig, H.: 'Enhancing performance of building integrated concentrating photovoltaic systems', PhD thesis, University of Exeter, 2015

29 Baig, H., Sellami, N., Mallick, T.K.: 'Trapping light escaping from the edges of the optical element in a concentrating photovoltaic system', *Energy Convers. Manage.*, 2015, **90**, pp. 238–246

30 Baig, H., Sarmah, N., Chemisana, D., *et al*.: 'Enhancing performance of a linear dielectric based concentrating photovoltaic system using a reflective film along the edge', *Energy*, 2014, **73**, (14), pp. 177–191

31 Shanks, K., Sarmah, N., Mallick, T.K.: 'The design and optical optimisation of a two stage reflecting high concentrating photovoltaic module using ray trace modelling'. 'PVSAT-9', 2013

32 Breault Research Organization: 'ASAP technical guide: scattering in ASAP'. Available at http://www.breault.com/sites/default/files/knowledge_base/brotg0922_scatter_1.pdf, accessed October 2015

33 Huang, C.K., Sun, K.W., Chang, W.-L.: 'Efficiency enhancement of silicon solar cells using a nano-scale honeycomb broadband anti-reflection structure', *Opt. Express*, 2012, **20**, (1), pp. A85–93

34 Zhou, G., He, J., Xu, L.: 'Antifogging antireflective coatings on Fresnel lenses by integrating solid and mesoporous silica nanoparticles', *Microporous Mesoporous Mater.*, 2013, **176**, pp. 41–47